EVOLUTION AT SMALL x

A. Donnachie

Department of Physics, Manchester University, Manchester M13 9PL, UK
ad@a35.ph.man.ac.uk

and P.V. Landshoff

Centre for Mathematical Sciences, Wilberforce Road, Cambridge CB3 0WA, UK
pvl@damtp.cam.ac.uk

(Received April 30, 2003)

Dedicated to Jan Kwieciński in honour of his 65th birthday

At present there is no correct theory of evolution of $F_2(x, Q^2)$ at small x. It is a mixture of hard and soft pomeron exchange and perturbative QCD very successfully describes the evolution of the hard-pomeron component. This allows the gluon density to be calculated. It is somewhat different from what is conventionally supposed, but it leads to a clean PQCD description of the data for the charm structure function. Perturbative QCD breaks down for the evolution of the soft-pomeron component of $F_2(x, Q^2)$.

PACS numbers: 13.60.Hb, 12.38.–t, 12.40.Nn

1. Introduction

The conventional treatment [1] [2] of evolution expands the DGLAP splitting matrix in powers of $\alpha_s(Q^2)$. As we will explain, this is almost certainly wrong at small x, and at present we have no correct theory. However, when we combine PQCD with Regge theory [3], this problem is partially solved and provides a very successful description of data, not only the complete proton structure function $F_2(x, Q^2)$ but also [4] its charm component $F_2^c(x, Q^2)$.

The proton's gluon density is larger at small x than is usually predicted, particularly at small Q^2. A consequence of this is that PQCD evolution cleanly and successfully describes charm production at small Q^2, even down to $Q^2 = 0$. See Fig. 1.

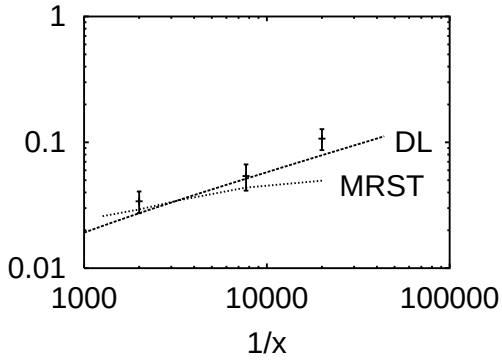


Fig. 1. Data [5] for $F_2^c(x,Q^2)$ at $Q^2 = 1.8\,\mathrm{GeV}^2$ with theoretical curves from references [1] and [4].

2. Regge theory — the two pomerons

At small x we make the fit [6]

$$F_2\left(x,Q^2\right) = f_0(Q^2)\,x^{-\varepsilon_0} + f_1(Q^2)\,x^{-\varepsilon_1} \tag{1}$$

at each Q^2 for which there are data. We fix $\varepsilon_1 = 0.0808$, the classical soft-pomeron value extracted from hadron–hadron scattering data [7,8]. It turns out that, although the data are now highly accurate, they do not constrain the value of ε_0 very closely. Good fits may be obtained with ε_0 anywhere between 0.35 and 0.5. We call this the "hard-pomeron" term. While varying ε_0 through its allowed range has little effect on the shape of the hard-pomeron coefficient function $f_0(Q^2)$, the large-Q^2 behaviour of the soft-pomeron coefficient function $f_1(Q^2)$ changes markedly; see Fig. 2.

For $\varepsilon_0 \approx 0.4$ the data make $f_1(Q^2)$ go to a constant at large Q^2. We assume [6] that $f_1(Q^2)$ has this behaviour and fit the available data for $x \leq 0.001$. When we made the fit we used data from ZEUS [9] at small Q^2

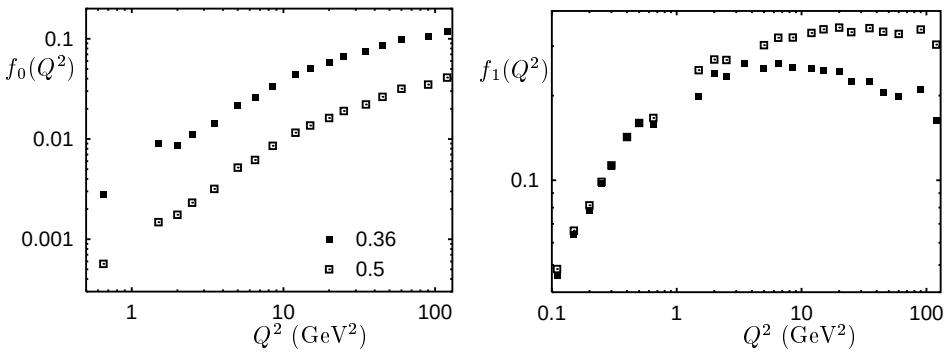


Fig. 2. The hard and soft pomeron coefficient functions extracted from data.

and from H1 [10] at larger Q^2. There are now data at large Q^2 also from ZEUS [11]. The best fit is now given by

$$f_0(Q^2) \;=\; A_0\,\frac{(Q^2)^{1+\varepsilon_0}}{\left(1+\frac{Q^2}{Q_0^2}\right)^{1+\varepsilon_0/2}}\,, \qquad f_1(Q^2) = A_1\,\frac{(Q^2)^{1+\varepsilon_1}}{\left(1+\frac{Q^2}{Q_1^2}\right)^{1+\varepsilon_1}}\,, \quad (2)$$

with

$$\begin{aligned} \varepsilon_0 \;&=\; 0.4075\,, \qquad \varepsilon_1 = 0.0808\,, \\ A_0 = 0.00227\,, \quad Q_0 \;&=\; 2.88\ \text{GeV}\,, \quad A_1 = 0.588\,, \quad Q_1 = 768\ \text{MeV}\,. \end{aligned} \quad (3)$$

See Fig. 3. We have already explained that the data do not constrain the value of ε_0 very closely. We have given the parameters to this accuracy because their errors are strongly correlated. This set of values gives a χ^2 per data point significantly less than 1.

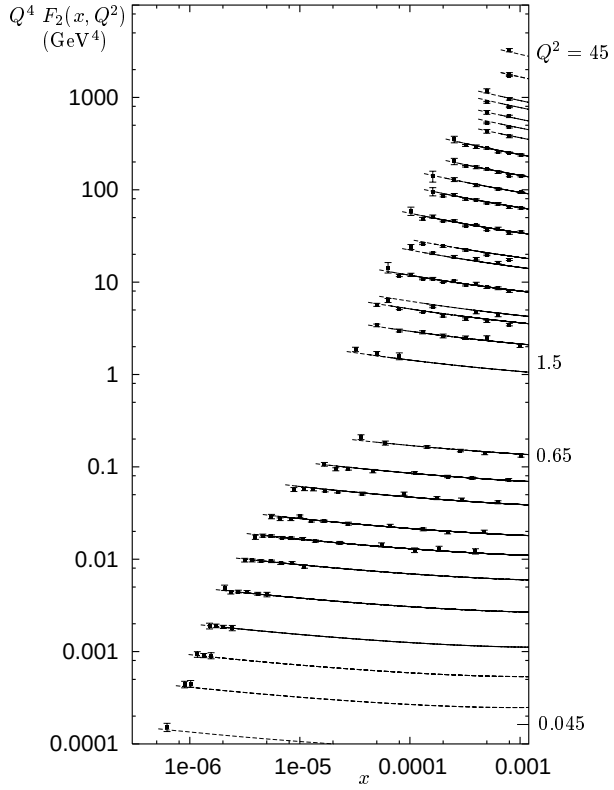


Fig. 3. Data from ZEUS [9, 11] and H1 [10] with two-pomeron fit [6]. Q^2 ranges from 0.045 to 45 GeV^2.

It is an extremely economical fit: we included in it also data for photoproduction (Fig. 9 below), which largely determine the value of A_1, so that there are just 4 free parameters. If we multiply (1) by $(1-x)^7$, which is a *very* crude way of ensuring that $F_2(x,Q^2)$ vanishes as $x \to 1$, and include a term corresponding to f_2, a_2 exchange, the fit agrees well with the data for larger x, even up to $Q^2 = 5000$ GeV^2: Fig. 4.

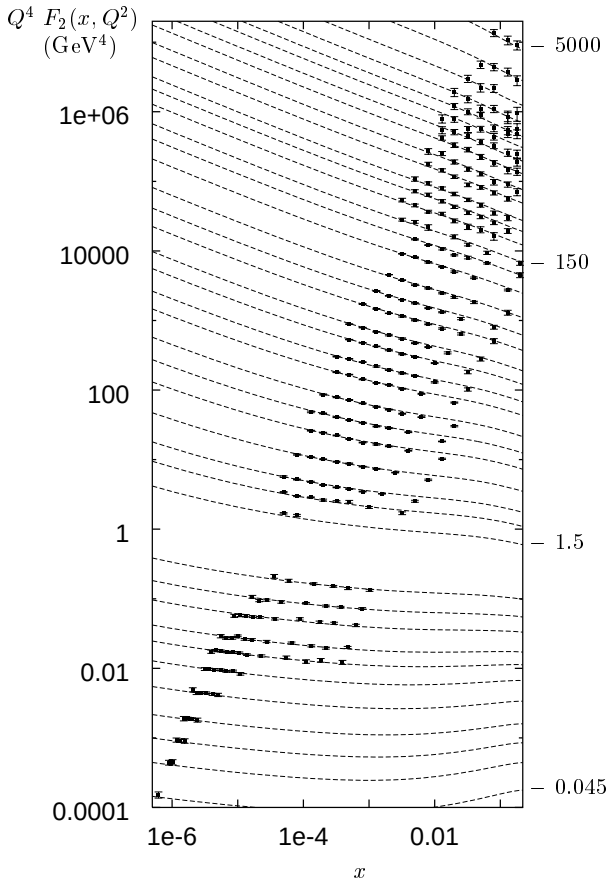


Fig. 4. The fit shown in Fig. 3 extended to larger x and Q^2.

If we try making a similar fit to the data [5] for the charm structure function, we find [6] that they correspond only to a hard-pomeron term. Further, the data are fitted well by assuming that the hard pomeron is flavour blind, so that for small x

$$F_2^c\left(x,Q^2\right) = 0.4\, f_0(Q^2)\, x^{-\varepsilon_0}\,, \tag{4}$$

where $f_0(Q^2)$ is defined in (1). The factor 0.4 is $\frac{4}{9}/(\frac{4}{9}+\frac{1}{9}+\frac{4}{9}+\frac{1}{9})$.

Fig. 5 shows

$$\sigma^c(W) = \frac{4\pi^2\alpha_{\rm EM}}{Q^2} F_2^c\left(x, Q^2\right)\Big|_{x=Q^2/(W^2+Q^2)}. \tag{5}$$

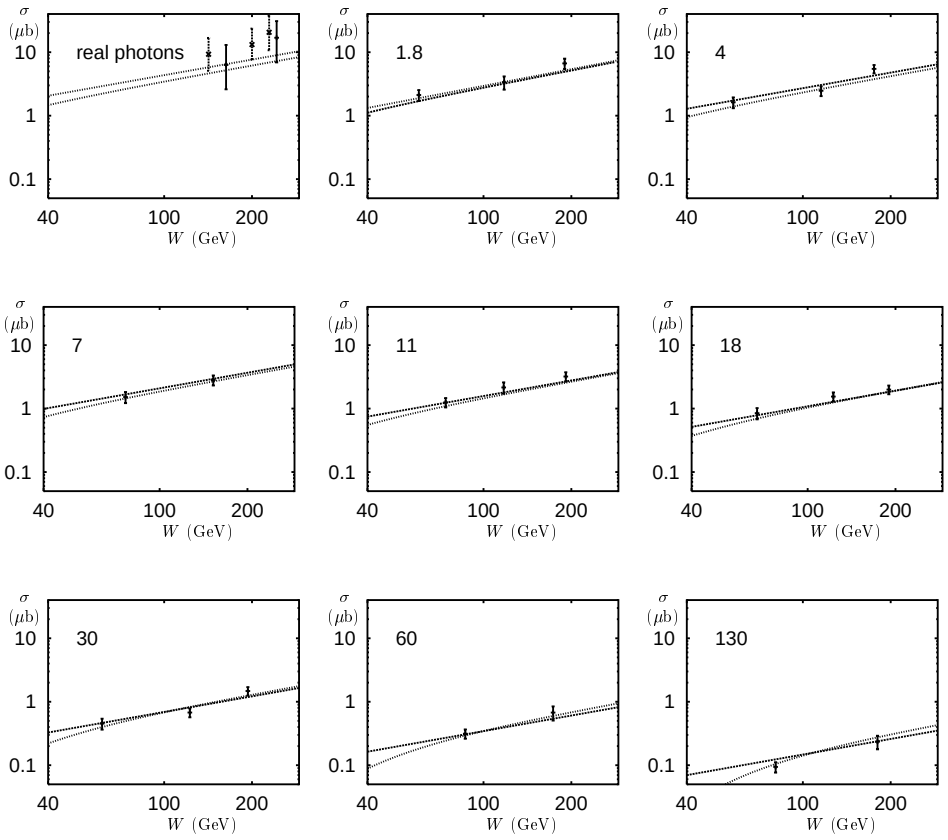


Fig. 5. Data [5] for $\sigma^c(W)$ defined in (5). The thick lines correspond to (4), which coincides with the output from DGLAP evolution, and the thin lines are from photon–gluon fusion.

3. The DGLAP equation

Define as usual the singlet parton densities

$$\boldsymbol{u}(x,t) = \begin{pmatrix} x\sum\limits_f (q_f + \bar{q}_f) \\ xg(x,t) \end{pmatrix}, \qquad t = \log\left(\frac{Q^2}{\Lambda^2}\right), \tag{6}$$

and take their Mellin transform with respect to x

$$\boldsymbol{u}(N,Q^2) = \int_0^1 dx\, x^{N-1}\boldsymbol{u}\left(x,Q^2\right)\ . \tag{7}$$

Then the DGLAP equation reads

$$\frac{\partial}{\partial t}\boldsymbol{u}(N,Q^2) = \boldsymbol{P}\left(N,\alpha_{\rm s}(Q^2)\right)\ \boldsymbol{u}(N,Q^2)\,, \tag{8}$$

where $\boldsymbol{P}(N,\alpha_{\rm s}(Q^2))$ is the Mellin transform of the splitting matrix.

The normal procedure is to expand $\boldsymbol{P}(N,\alpha_{\rm s}(Q^2))$ in powers of $\alpha_{\rm s}(Q^2)$. However, this is illegal when N is close to 0. This is well known. Compare, for example, the analogous expansion of the function

$$\begin{aligned}\psi(N,\alpha_{\rm s})) &= \sqrt{N^2+\alpha_{\rm s}} - N \\ &= \frac{\alpha_{\rm s}}{2N} - \frac{\alpha_{\rm s}^2}{8N^3} + \ldots\end{aligned} \tag{9}$$

Although each term in the expansion is singular at $N=0$, the function ψ is not: the expansion is valid only for $|N| > \alpha_{\rm s}$. Similarly, the terms in the expansion of $\boldsymbol{P}(N,\alpha_{\rm s}(Q^2))$ have singularities at $N=0$ which are surely not present in $\boldsymbol{P}(N,\alpha_{\rm s}(Q^2))$ itself. Indeed, it is likely that $\boldsymbol{P}(N,\alpha_{\rm s}(Q^2))$ has no relevant N-plane singularities at all.

At any given Q^2, expanding the splitting matrix in powers of the QCD coupling becomes invalid when one goes to sufficiently small x.

At present, we have no other way to calculate. Luckily, if we introduce the two-pomeron parametrisation of the data we can partially rescue the situation. A fixed-power behaviour

$$\boldsymbol{u}(x,t) \sim x^{-\varepsilon}\,, \tag{10}$$

as occurs for each of the terms in (1) corresponds to

$$\boldsymbol{u}(N,Q^2) \sim \frac{\boldsymbol{f}(Q^2)}{N-\varepsilon}\,, \qquad\qquad \boldsymbol{f}(Q^2) = \begin{pmatrix} f_q(Q^2) \\ f_g(Q^2)\end{pmatrix}\ . \tag{11}$$

If we insert this behaviour into the DGLAP equation (8) and equate the coefficient of the pole at $N=\varepsilon$ on each side of the equation, we find an exact equation that describes how $\boldsymbol{f}(Q^2)$ evolves with Q^2

$$\frac{\partial}{\partial t}\boldsymbol{f}(Q^2) = \boldsymbol{P}\left(N=\epsilon,\alpha_{\rm s}(Q^2)\right)\ \boldsymbol{f}(Q^2)\,. \tag{12}$$

4. DGLAP evolution

To calculate the evolution of the soft-pomeron term in (1) we need $\boldsymbol{P}(N, \alpha_s(Q^2))$ at $N = 0.0808$. This is dangerously close to $N = 0$; we cannot make the expansion in powers of α_s and do not know how to calculate the splitting matrix at this value of N. But for the hard-pomeron term we need $\boldsymbol{P}(N, \alpha_s(Q^2))$ for $N \approx 0.4$, which is safely away from $N = 0$ and so the expansion should be valid.

In order to solve the evolution equation (12) for the hard-pomeron coefficient functions $f_q(Q^2)$ and $f_g(Q^2)$, we chose $Q^2 = 20$ GeV^2 as our starting value. It does not matter what value we take, as long as it is not too small. We also assumed that, at this value of Q^2, the conventional DGLAP analysis of the data is correct for values of x down to about 0.01. That is, we assumed that the value of $g(x = 0.01, Q^2 = 20)$ extracted from the data by MRST [1] or CTEQ [2] is correct. Further because, as we have seen, the charm structure function is entirely hard-pomeron exchange at small x and because, as is well known, it is directly related to the gluon density, we deduce that $g(x, Q^2)$ at small x is entirely hard-pomeron exchange. Therefore, we know the value of $f_g(Q^2)$ at $Q^2 = 20$. For the value of $f_q(Q^2)$ at $Q^2 = 20$ we go to our fit to the data, that is we use (2) and (3).

We then used (12) to evolve away from $Q^2 = 20$, in both directions. The result is rather astonishing: although the phenomenological function $f_0(Q^2)$ in (2) rises at large Q^2 as a power of Q^2, while the solution to (12) rather rises as a power of $\log Q^2$, the two are in extraordinarily good numerical agreement over a wide range of Q^2. This is shown in Fig. 6. We took 4 flavours, with $\Lambda_{\rm LO} = 140$ MeV. We have found [3] that the output is the almost same whether we work to leading order in the coupling or next-to-leading.

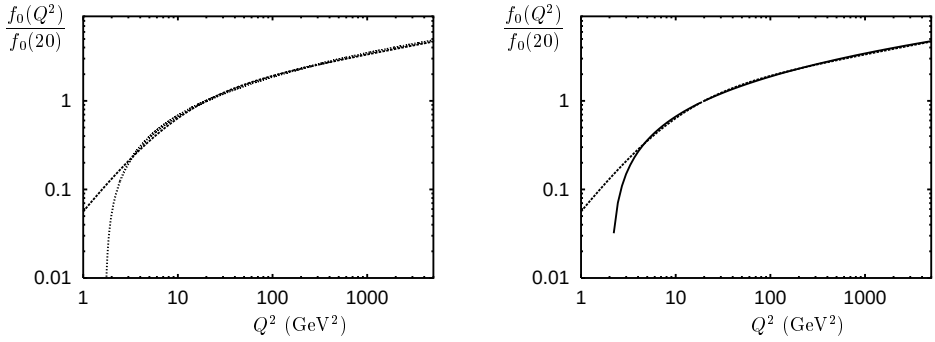


Fig. 6. LO and NLO calculations of the hard-pomeron coefficient function, together with the phenomenological fit (2).

So, for Q^2 greater than about $5\,\mathrm{GeV}^2$ perturbative QCD describes the evolution of the hard-pomeron component of $F_2(x,Q^2)$ extremely well. This is a significant success both for PQCD and for the two-pomeron description of $F_2(x,Q^2)$. It is no surprise that perturbative evolution breaks down at small Q^2; the DGLAP equation is supposed to be valid only for sufficiently large Q^2.

5. Gluon density

According to what we have said, the proton's gluon density is

$$xg\left(x,Q^2\right) = f_g(Q^2)x^{-\varepsilon_0}\phi\left(x,Q^2\right)\,, \tag{13}$$

where $\phi(0,Q^2)=1$ and $\phi(x,Q^2)\to 0$ as $x\to 1$. A good numerical fit to the LO $f_g(Q^2)$ in the range $5<Q^2<1000$ is given by

$$f_g(Q^2) = 0.32\frac{(Q^2)^{1+\varepsilon_0}}{(1+Q^2/1.4)^{1+\varepsilon_0/2}}\,. \tag{14}$$

At $Q^2=20$ GeV^2 the MRST or CTEQ LO gluon density is well described by $\phi(x,Q^2=20)=(1-x)^6$. Fig. 7 compares our gluon distribution in LO with those of MRST and CTEQ at two values of Q^2. The differences are evident and become even more pronounced in NLO, where our distribution is much the same but those of MRST and CTEQ are rather smaller and significantly less steep.

In NLO, our gluon distribution turns out [3] to be almost the same as in LO. This is because we use the DGLAP splitting matrix only at $N\approx 0.4$, where all but one of its elements are almost equal in LO and NLO. As x

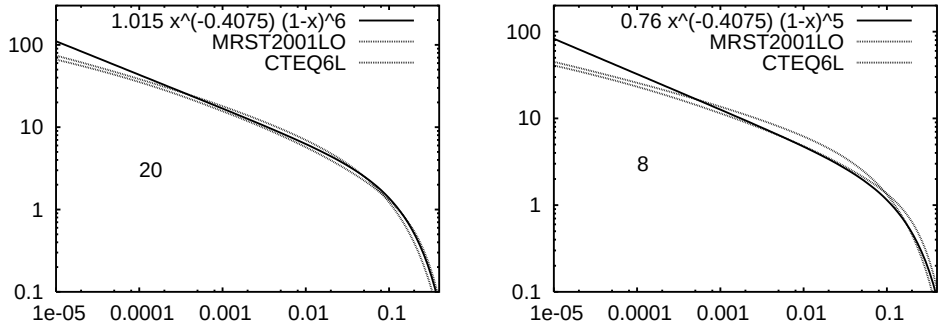


Fig. 7. The LO gluon density $xg(x,Q^2)$ at $Q^2=20$ GeV^2 and 8 GeV^2. The CTEQ and MRST curves are from the Durham Data Base [13].

decreases, the conventional analysis involves the splitting matrix at progressively smaller values of N, where its elements are no longer the same in LO and NLO. At very small x the conventional analysis involves very small N, where it becomes illegal to use the perturbative expansion of the splitting matrix.

At $Q^2 = 200$ GeV^2 and $x = 0.0001$ our gluon distribution is twice as large as that of MRST or CTEQ. The fact that our NLO gluon density is larger than the conventional one at small x will be significant for experiments at the LHC.

The cleanest window on the gluon density will be provided by good data for the longitudinal structure function $F_{\rm L}(x, Q^2)$. Those data that exist depend on some assumed parametrisation to separate $F_{\rm L}$ from F_2, for example reference [14]. Fig. 8 shows that already at $Q^2 = 20$ GeV^2 there is a clear difference between our prediction and that of MRST.

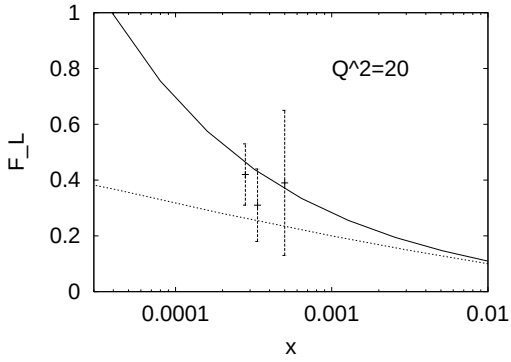


Fig. 8. The longitudinal structure function at $Q^2 = 20$ GeV^2: data from H1 [14] with our prediction (upper curve) and that of MRST [1].

6. Charm production

It is standard [15–17] that at small Q^2 the charm structure function $F_2^c(x, Q^2)$ should be calculated from photon-gluon fusion, $\gamma^* g \to c\bar{c}$, to some fixed order in $\alpha_{\rm s}$. This calculation introduces some assumed value for the charmed-quark mass m_c. At large Q^2 a resummation to all orders in $\alpha_{\rm s}$ is needed, because of the presence of factors of powers of $\log Q^2/m_c^2$. This resummation is achieved by changing at large Q^2 to the output from DGLAP evolution, where the charmed quark mass can now be neglected. The two calculations have to be matched at some value of Q^2. The usual matching is done at a rather small value of Q^2, of the order of m_c^2, and is sensitive to exactly what value is chosen.

The thin lines in Fig. 5 show the result of the LO calculation of photon–gluon fusion with our gluon density and $m_c = 1.3$ GeV. The results of an NLO calculation are almost the same, if we increase m_c to 1.6 GeV. This calculation used the code of [18, 19] with our gluon distribution and m_c as a free parameter. The thick lines in the figure are the fit (4) which, as we have shown, agrees well with the output from DGLAP evolution for Q^2 greater than about $5\,\mathrm{GeV}^2$. So in our approach the two calculations match well over a range of Q^2, from about 5 to $50\,\mathrm{GeV}^2$.

7. The hard pomeron

It used to be a central tenet of high energy physics that scattering amplitudes are analytic functions of all their variables [20]. A consequence of this is that a singularity that is present in an amplitude at large Q^2 survives when one goes to $Q^2 = 0$. In particular, if the hard pomeron is present at large Q^2 it should also be present at $Q^2 = 0$.

This view is strongly reinforced by the charm-production data shown in Fig. 5. The W dependence at $Q^2 = 0$ is the same as at higher Q^2. The hard pomeron is not generated by PQCD evolution, though the evolution makes it relatively more important as Q^2 increases. Thus, in the fit we have described to $F_2(x, Q^2)$, there is a small hard-pomeron component already at small Q^2, though its significance is masked by the much larger soft pomeron component. Both grow with increasing Q^2, but the hard-pomeron component grows faster, and at each small value of x it dominates at sufficiently large Q^2.

Fig. 9 shows the data for the photoproduction cross section. The curve is our old fit [7,8], with no hard-pomeron term. The data are not yet good enough to test whether the fit is adequate or whether an extra component is needed such that indeed the hard pomeron is present already at $Q^2 = 0$. The same statement may be made of the LEP data [21,22] for $\sigma^{\gamma\gamma}$, which depend too heavily on Monte Carlo simulations that correct for poor acceptance to reach any conclusion.

If the hard pomeron is present in the total cross section for photon collisions, is the same true for pp collisions? While probably the hard pomeron couples to a small object such as the photon with larger relative strength than to a large object such as the proton, there is some prospect that LHC data will show that there is a hard-pomeron component to σ^{pp}.

What is the hard pomeron? Everybody agrees that the sharp rise in $F_2(x, Q^2)$ at small x discovered at HERA is a consequence of gluon exchange. Our own belief is that it is caused by glueball exchange and that the hard and soft pomerons are just glueball Regge trajectories. There is some evidence that this is true for the soft pomeron: there is a 2^{++} glueball candidate at

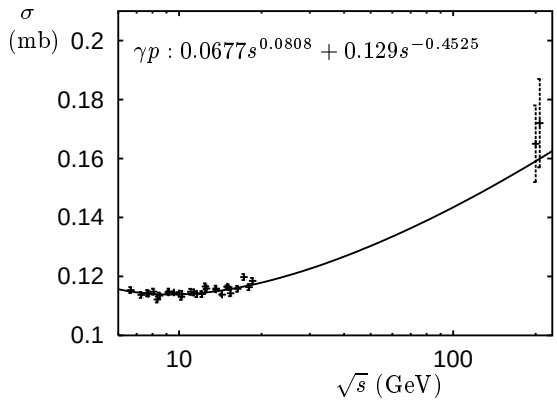


Fig. 9. γp total cross section; the curve takes account of the exchange of the soft pomeron, f_2 and a_2.

1926 MeV, exactly the right mass to be on the soft-pomeron trajectory [23]. Another 2^{++} glueball candidate [25], at 2350 MeV, could well be on the hard-pomeron trajectory [24].

At one time there was a hope that the power ε_0 of $1/x$, which is the hard-pomeron-exchange term, might be calculated from the BFKL and, therefore, that it is a perturbative effect. The soft-pomeron trajectory surely cannot be calculated from perturbative QCD. It may be that the glueballs on the hard-pomeron trajectory are heavy enough for their masses to be calculated from PQCD though, with the problems that have arisen with the BFKL equation, it is far from clear that PQCD can be used to calculate the intercept $1 + \varepsilon_0$ of the trajectory.

8. Summary

- The conventional approach to evolution needs modifying at small x.
- It can be corrected if we combine it with Regge theory.
- But only partly — we can only treat the hard-pomeron part.
- This is enough to extract the gluon distribution.
- The gluon distribution is larger at small x than has so far been supposed.
- It gives a good description of charm production.
- We want good data for the longitudinal structure function.

This research was supported in part by PPARC.

REFERENCES

[1] A.D. Martin, R.G. Roberts, W.J. Stirling, R.S. Thorne, *Eur. Phys. J.* **C18**, 117 (2000).

[2] CTEQ Collaboration: J. Pumplin *et al.*, *J. High Energy Phys.* **0207**, 012 (2002).

[3] A. Donnachie, P.V. Landshoff, *Phys. Lett.* **B533**, 277 (2002).

[4] A. Donnachie, P.V. Landshoff, *Phys. Lett.* **B550**, 160 (2002).

[5] ZEUS Collaboration: J. Breitweg *et al.*, *Eur. Phys. J.* **C12**, 35 (2000).

[6] A. Donnachie, P.V. Landshoff, *Phys. Lett.* **B518**, 63 (2001).

[7] A. Donnachie, P.V. Landshoff, *Phys. Lett.* **B296**, 227 (1992).

[8] A. Donnachie, H.G. Dosch, P.V. Landshoff, O. Nachtmann, *Pomeron Physics and QCD*, Cambridge University Press, 2002, see `www.damtp.cam.ac.uk/user/pvl/QCD/`.

[9] ZEUS Collaboration: J. Breitweg *et al.*, *Phys. Lett.* **B407**, 432 (1997).

[10] H1 Collaboration: C. Adloff *et al.*, *Nucl. Phys.* **B497**, 3 (1997).

[11] ZEUS Collaboration: S. Chekanov *et al.*, `hep-ex/0208040`.

[12] R.K. Ellis, W.J. Stirling, B.R. Webber, *QCD and Collider Physics*, Cambridge University Press, 1996.

[13] Durham Data Base (`durpdg.dur.ac.uk/hepdata/pdf.html`).

[14] H1 Collaboration: C. Adloff *et al.*, *Eur. Phys. J.* **C21**, 33 (2001).

[15] M.A.G. Aivazis, J.C. Collins, F.I. Olness, W-K. Tung, *Phys. Rev.* **D50**, 3102 (1994).

[16] R.S. Thorne, R.G. Roberts, *Phys. Lett.* **B421**, 303 (1998).

[17] M. Buza, Y. Matiounine, J. Smith, W.L. van Neerven, *Eur. Phys. J.* **C1**, 301 (1998).

[18] E. Laenen, S. Riemersma, J. Smith, W.L. van Neerven, *Nucl. Phys.* **B392**, 162 (1993).

[19] S. Riemersma, J. Smith, W.L. van Neerven, *Phys. Lett.* **B347**, 143 (1995).

[20] R.J. Eden, P.V. Landshoff, D.I. Olive, J.C. Polkinghorne, *The Analytic S-Matrix*, Cambridge University Press, 2002.

[21] OPAL Collaboration: G. Abbiendi *et al.*, *Eur. Phys. J.* **C14**, 199 (2000).

[22] L3 Collaboration: M. Acciari *et al.*, *Phys. Lett.* **B519**, 33 (2001).

[23] WA91 Collaboration: S. Abatzis *et al.*, *Phys. Lett.* **B324**, 509 (1994).

[24] A. Donnachie, P.V. Landshoff, *Phys. Lett.* **B437**, 408 (1998).

[25] WA102 Collaboration: D. Barberis *et al.*, *Phys. Lett.* **B440**, 225 (1998).